CrossMark

ARTICLE

Retinopathy with central oedema in an INS^{C94Y} transgenic pig model of long-term diabetes

Kristina J. H. Kleinwort[1] · Barbara Amann[1] · Stefanie M. Hauck[2,3] · Sieglinde Hirmer[1] ·
Andreas Blutke[4] · Simone Renner[3,5] · Patrizia B. Uhl[1] · Karina Lutterberg[1] ·
Walter Sekundo[6] · Eckhard Wolf[3,5] · Cornelia A. Deeg[7]

Abstract

Aims/hypothesis Diabetic retinopathy is a severe complication of diabetes mellitus that often leads to blindness. Because the pathophysiology of diabetic retinopathy is not fully understood and novel therapeutic interventions require testing, there is a need for reliable animal models that mimic all the complications of diabetic retinopathy. Pig eyes share important anatomical and physiological similarities with human eyes. Previous studies have demonstrated that INS^{C94Y} transgenic pigs develop a stable diabetic phenotype and ocular alterations such as cataracts. The aim of this study was to conduct an in-depth analysis of pathological changes in retinas from INS^{C94Y} pigs exposed to hyperglycaemia for more than 2 years, representing a chronic diabetic condition.

Methods Eyes from six INS^{C94Y} pigs and six age-matched control littermates were analysed via histology and immunohistochemistry. For histological analyses of retinal (layer) thickness, sections were stained with H&E or Mallory's trichrome. For comparison of protein expression patterns and vessel courses, sections were stained with different antibodies in immunohistochemistry. Observed lesions were compared with reported pathologies in human diabetic retinopathy.

Results INS^{C94Y} pigs developed several signs of diabetic retinopathy similar to those seen in humans, such as intraretinal microvascular abnormalities, symptoms of proliferative diabetic retinopathy and central retinal oedema in a region that is cone rich, like the human macula.

Conclusions/interpretation The INS^{C94Y} pig is an interesting model for studying the pathophysiology of diabetic retinopathy and for testing novel therapeutic strategies.

✉ Cornelia A. Deeg
Cornelia.Deeg@uni-marburg.de

[1] Institute of Animal Physiology, Department of Veterinary Sciences, LMU Munich, Munich, Germany

[2] Research Unit Protein Science, Helmholtz Zentrum München, German Research Centre for Environmental Health GmbH, Munich, Germany

[3] German Centre for Diabetes Research (DZD), Neuherberg, Germany

[4] Institute of Veterinary Pathology, Centre for Clinical Veterinary Medicine, LMU Munich, Munich, Germany

[5] Molecular Animal Breeding and Biotechnology, Gene Centre, LMU Munich, Munich, Germany

[6] Department of Ophthalmology, Philipps University of Marburg, Marburg, Germany

[7] Experimental Ophthalmology, Philipps University of Marburg, Baldingerstrasse, D-35033 Marburg, Germany

Abbreviations

AQP	Aquaporin
DBA	*Dolichos biflorus* agglutinin
GS	Glutamine synthetase
LEL	*Lycopersicon esculentum* lectin
NEFH	Neurofilament heavy chain
SMA	Smooth muscle actin

Introduction

Individuals with diabetes mellitus are showing an increasing incidence of diabetic retinopathy, a severe complication that often results in blindness [1]. A recent population-based study reported that 13% of individuals newly diagnosed (screening-detected) with type 2 diabetes already showed signs of diabetic retinopathy [2]. Visual impairment is primarily a sequelae to macular oedema, an exudative fluid accumulation in the macula that affects one in 15 individuals with diabetes [3]. Currently, more than 20 million individuals worldwide suffer from this form of sight-threatening diabetic retinopathy and numbers are rising exponentially with the incidence of diabetes [3]. To date, the pathophysiology of diabetic retinopathy is not fully understood, and the translational value of established animal models (e.g. for impairment of cone function in the macula) is limited by differences in retinal architecture and cellular composition in the central area [4, 5]. Nevertheless, rodent models have great value for studying pathophysiological matters such as vasogenic oedema formation in streptozotocin-induced diabetic rats, or the direct effects of drugs on retinal vascular function and thickness [6, 7].

Human vision depends heavily on the macula, an area with increased density of cones, cone bipolar cells and ganglion cells, providing high optical resolution [8]. Many mammals possess a specialised retinal region comparable with the macula, with an increased density of cones, ganglion cells and bipolar cells, either in the form of a roughly circular area centralis or as a horizontal visual streak [8]. In contrast to rodents, the cone density observed in the visual streak of the pig retina (20,000–40,000 cones/mm^2) [9] is quite similar to that in the outer regions (non-foveal region) of the human macula (20,000–40,000 cones/mm^2) [10].

In general, pig and human eyes are similar in their size, anatomy and physiological characteristics. As animals with high life expectancy, the use of pigs enables the study of the long-term pathophysiological consequences of chronic metabolic disturbances [11]. The INS^{C94Y} transgenic pig is a novel large-animal model of diabetes mellitus that is characterised by impaired insulin secretion, decreased beta cell mass and permanent hyperglycaemia [12]. Cataracts develop within the first week of life in these INS^{C94Y} pigs, indicating an ocular pathophysiological phenotype [11]. Since this model could potentially be useful for testing novel therapeutic strategies counteracting diabetic retinopathy and offers the opportunity to investigate the effects of long-term hyperglycaemia on visual function and the development of retinal oedema, we aimed to characterise the ocular phenotype of long-term diabetic INS^{C94Y} pigs, particularly in the retina. Observed changes were related to disease characteristics in humans in

Fig. 1 Changes in retinas of INS^{C94Y} pigs. Enlargement of layers, especially of the nerve fibre/ganglion cell layer. Representative images (Mallory's trichrome staining) of retinal layer size in (**a**) a control pig; and (**b**) an INS^{C94Y} pig with a distance of 2 mm to the optic nerve (×20 magnification). (**c**) Measurement of overall retinal thickness (nerve fibre/ganglion cell layer to outer limiting membrane) at different distances from the optic nerve revealed statistically significant differences between control (white bars) and INS^{C94Y} (black bars) pigs. *$p < 0.05$, **$p < 0.01$, ***$p < 0.001$ vs control. (**d**) Mean thickness measurement of different retinal layers at a 2 mm distance from the optic nerve head in control (white bars) and INS^{C94Y} (black bars) pigs ($n = 6$ per group, four measurements per layer). Data are means ± SD. ***$p < 0.001$ vs control. (**e**) An intraretinal vessel in a control pig and (**f**) an irregularly shaped vessel in an INS^{C94Y} pig (H&E staining). Smooth muscle cells in the vessel walls (SMA, red) of (**g**) control pigs and (**i**) INS^{C94Y} pigs. Basolateral luminal surface (DBA, green) in (**h**) control and (**j**) INS^{C94Y} pigs. (**k**) Nerve fibre/ganglion cell layer in a control pig with a large vessel and (**l**) disruption of the nerve fibre/ganglion cell layer with an irregularly shaped vessel (arrow) in an INS^{C94Y} pig (Mallory's stain) (**e–l**: scale bars, ±20 μm). Stars indicate the vessel lumen. ILM, inner limiting membrane; INL, inner nuclear layer; IPL, inner plexiform layer; NFL/GCL, nerve fibre/ganglion cell layer; ONL, outer nuclear layer; OPL, outer plexiform layer. PR, photoreceptors; RPE, retinal pigment epithelium ▶

order to prove the translational quality of this novel model for diabetic retinopathy pathophysiology.

Methods

Animal model, sample preparation for histology and immunohistochemistry The generation of and main pathophysiological findings in INS^{C94Y} pigs have been described previously [11, 13]. For this study, we used six INS^{C94Y} male and female pigs and six age-matched control littermates (ten pigs aged 24 months and two aged 40 months) generated at the Molecular Animal Breeding and Biotechnology, Gene Centre, LMU Munich, in their facility in Oberschleissheim, Germany. All animal experiments were performed according to the German Animal Welfare Act and were permitted by local authorities (ROB 55.2-1-54-2532-68-11). Animals were housed under controlled conditions, with a once-a-day feeding regimen and free access to water. Continuous glucose monitoring was performed using the Guardian REAL-Time System (Medtronic, Meerbusch, Germany) with a glucose sensor inserted subcutaneously behind the ear and transfer of collected data via a connected transmitter to an external computer. Blood glucose levels were determined once or twice daily using a glucometer. In addition, fructosamine levels were monitored as an adequate evaluation of medium-term glucose control in pigs [14, 15]. Fructosamine levels were determined in EDTA-plasma using an AU480 Autoanalyzer and an adapted reagent kit from Beckman-Coulter (Krefeld, Germany). At the time point of sampling of the eyes, mean fructosamine
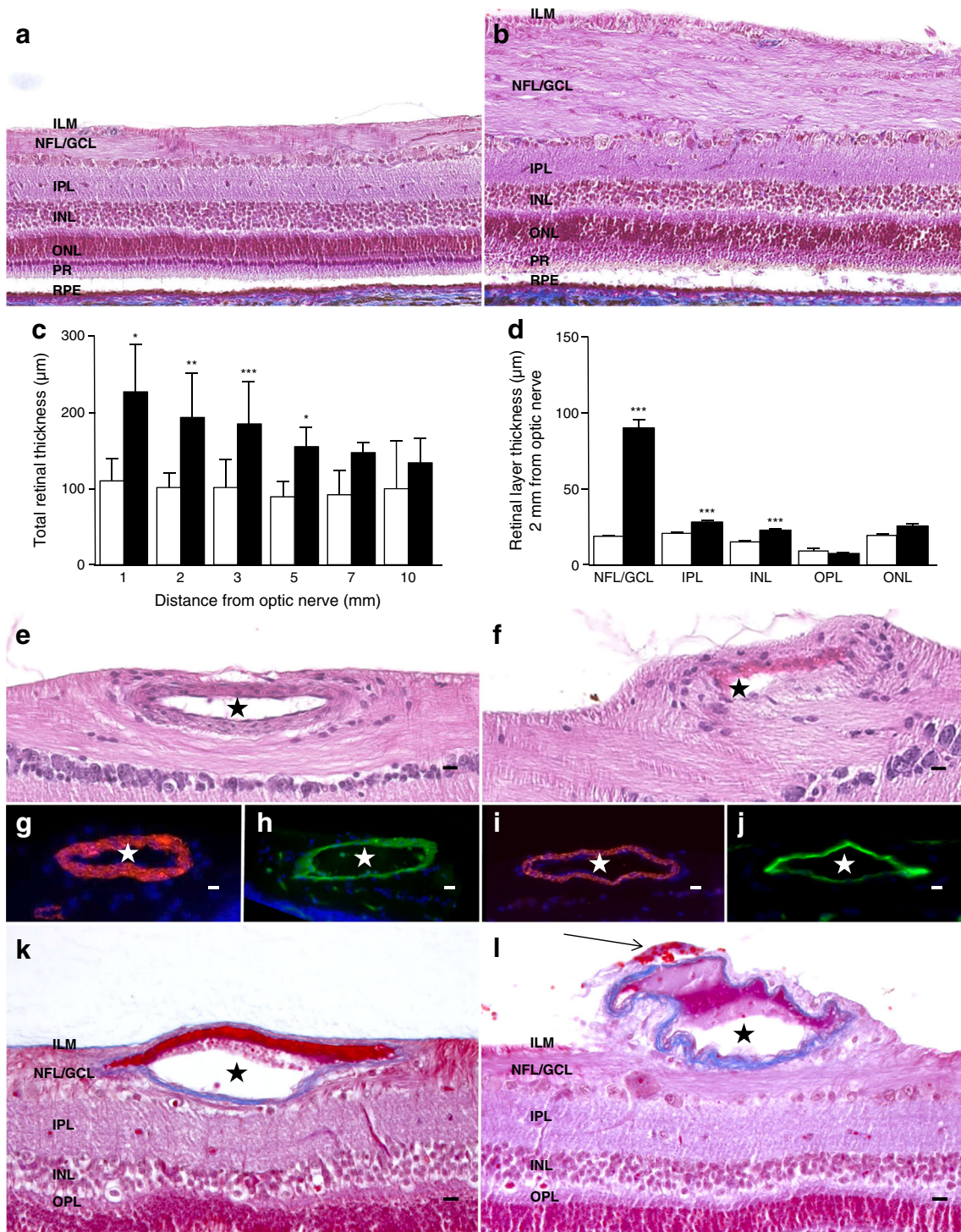
levels were 380.17 ± 41.50 μmol/l in control pigs and 684.83 ± 61.96 μmol/l in INS^{C94Y} pigs (Student's *t* test, *p* < 0.0001), confirming a chronic hyperglycaemic state in the INS^{C94Y} pigs. Animals were euthanised after 24 or 40 months, respectively. Immediately after enucleation, eyes were dissected

to obtain sections containing low and high ganglion cell density areas [16] of the porcine retina, as recently described [12]. Briefly, a sagittal section was cut through the optic nerve, dividing the eye cup into temporal and nasal halves to obtain cross-sections representing central and peripheral retinas, characterised by

4000–5000 (central) and 500–1000 ganglion cells per mm^2 (periphery), respectively [16]. In pigs, this area of high cone density, called the visual streak, is a broad horizontal band situated around and above the optic nerve. The highest density, with 40,500 cones per mm^2, can be found in a small area of the visual streak above the optic nerve in the nasal direction [9]. This area has cone densities comparable with those in the human macula and is preferentially damaged in diabetic retinopathy [3, 10]. The temporal part was fixed in formalin, and the nasal part in Bouin's solution. Dehydration, embedding, cutting and mounting on coated slides were performed as previously described [17].

Histology and immunohistochemistry, measurement of layer thickness and counting of blood vessel section profiles Specimens from all six INS^{C94Y}pigs and all six control pigs were used for all stainings. For histological analyses, sections were deparaffinised, rehydrated and stained with H&E or Mallory's trichrome [17]. For immunohistochemistry, heat antigen retrieval was performed [17]. The following primary antibodies were used: monoclonal mouse anti-glutamine synthetase (GS; 1:1500; BD Biosciences, Heidelberg, Germany); mouse anti-smooth muscle actin (SMA; 1:50; Sigma-Aldrich, Taufkirchen, Germany); FITC-labelled lectins *Dolichos biflorus* agglutinin (DBA) and *Lycopersicon esculentum* lectin (LEL) (all 3 μg/ml; Vector, Burlingame, CA, USA); polyclonal rabbit anti-phosphorylated (p)IRS1 (Ser302-307; 1:500; Merck Millipore, Darmstadt, Germany); rabbit anti-aquaporin 4 (AQP4; 1:200; Alomone, Jerusalem, Israel); polyclonal rabbit anti-pIRS1 (Tyr895; 1:100; Merck Millipore); monoclonal rat anti-S-opsin (neat) [17], polyclonal rabbit anti-cone arrestin, (1:10,000) [18] and polyclonal rabbit anti-neurofilament heavy chain (NEFH; 1:500; Sigma-Aldrich). Fluorescence-labelled (488 or 568) secondary antibodies to mouse and rabbit IgG heavy and light chain (1:500; Invitrogen, Karlsruhe, Germany) and to rat IgG2c (1:200, Invitrogen, Karlsruhe, Germany) were used [18]. Images were recorded using a Leica DMR (Leica, Wetzlar, Germany) or Axio Vision Imager M1 (Zeiss, Jena, Germany). All stainings included appropriate isotype controls. For quantification of retinal layer thickness, complete sections were scanned with a C9600-12 scanner and analysed using NDP.view version 2.4.26 (Hamamatsu, Herrsching am Ammersee, Germany). Retinal layer thickness was measured at different defined distances from the optic nerve. All measurements were performed independently by two researchers in separate experiments. The number of vessel section profiles was quantified over a length of 1 mm by counting LEL-positive areas.

Statistics Retinal layer thickness measurements (in μm) are presented as means ± SD. The Mann–Whitney U test was used to compare retinal layer thicknesses (complete and single layers). Student's t test was used to compare vessel numbers and fructosamine levels between control and diabetic INS^{C94Y}pigs. The significance threshold was $p < 0.05$ in all analyses.

Results

Retinal layer thickness is substantially increased in INS^{C94Y}pigs, especially in the nerve fibre/ganglion cell layer
Measurements of retinal thickness revealed significant changes in INS^{C94Y}pigs (Fig. 1a–c). Total retinal thickness was measured at different distances from optic nerve and compared between control and diabetic INS^{C94Y}animals. There was a significant increase in total retinal thickness in INS^{C94Y}animals, especially 2 and 3 mm from the optic nerve (Fig. 1c). The retinal thickening in INS^{C94Y}pigs could be attributed to the nerve fibre/ganglion cell layer, as well as the inner plexiform and inner nuclear layers (Fig. 1d).

INS^{C94Y}pigs have intraretinal vascular abnormalities that are typical of diabetic retinopathy Several intraretinal vessels of INS^{C94Y}pigs were irregular and coiled (Fig. 1a–k: control pigs; Fig. 1b–l: diabetic INS^{C94Y} pigs), with changes in endothelial cells and the inner membrane (Fig. 1g–j). Loop formation of capillaries in the retinas of INS^{C94Y}pigs (Fig. 1k: control pig; Fig. 1l: diabetic INS^{C94Y} pig) was detectable. In addition, extraretinal haemorrhage was visible in the gross pathology of the fundus of diabetic INS^{C94Y}pigs, with erythrocytes in the vitreous (Fig. 1l, arrow). Disruption of the inner limiting membrane (Fig. 1l, arrow) and the nerve fibre/ganglion cell layer in INS^{C94Y}pigs resulted in cotton-wool spots.

Findings in the eyes of diabetic INS^{C94Y}pigs indicate changes in the intraretinal vessel course and the function of colour vision Mature cataracts were absent in control pigs (Fig. 2a, c) but present in the lenses of all six INS^{C94Y}pigs examined (Fig. 2b, d). Some lenses had additional overlayings, and globules of cataract-typical eosinophilic material could be located between lens fibres (Fig. 2d). Examination of intraretinal vessels showed tortuous vessels and loop formations in the retinas of INS^{C94Y}pigs (Fig. 2e, f). This was confirmed by a significant increase in the number of blood vessel section profiles in the retinas of INS^{C94Y}pigs compared with control animals (Fig. 2g, h). Differences in cone arrestin expression levels were detectable in the retinas of all six INS^{C94Y}pigs (Fig. 2j–p) compared with non-transgenic control pigs (Fig. 2i–o) despite morphologically intact cones in these

animals (Fig. 2j). S-opsin expression was similar between both groups ($n = 6$ in each group), but cone arrestin expression was markedly reduced in all INS^{C94Y} pigs (Fig. 2n, p).

Altered abundance and localisation of cell metabolism and water-clearance proteins in INS^{C94Y} pig retinas To investigate potential differences in insulin signal transduction, we examined phosphorylation of IRS1, which is regulated by insulin. Loss of insulin signalling and IRS proteins is instrumental to the development and/or progression of diabetic complications [19]. We could not detect phosphorylation of serine 302_307 residues in the retinas of either control (Fig. 3c) or INS^{C94Y} (Fig. 3d) pigs, but we did observe enhanced phosphorylation of IRS1 on tyrosine residue 895 in diabetic INS^{C94Y} pigs (Fig. 3f) in contrast to control pigs (Fig. 3e).

An increase in NEFH abundance indicated an enlargement of neurons/axons in the nerve fibre/ganglion cell layer (Fig. 3g, h), and not of the Müller glial endfeet (Fig. 3k, l). The main water channel of the retina, AQP4 (Fig. 3m, n), changed from a Müller glial endfeet pattern in control retinas (Fig. 3m) to an entire Müller glial cell accented expression pattern in diabetic INS^{C94Y} pigs, with an accentuation of the endfeet at the inner limiting membrane (Fig. 3n, p).

Long-term diabetes in INS^{C94Y} pigs is associated with signs of severe diabetic retinopathy Diabetic retinopathy in humans is graded based on intraretinal microvascular abnormalities and the classification into non-proliferative or proliferative diabetic retinopathy [20]. When retinopathy additionally affects the macular region it is designated as diabetic maculopathy and, with additional retinal oedema in this region, it is specified as diabetic macular oedema [20]. There are many animal models representing different clinical features of diabetic retinopathy, but none of them replicates all features [21]. In this study, long-term diabetic INS^{C94Y} pigs developed many important signs of severe complications, such as extraretinal haemorrhages and cotton-wool spots resulting from focal disruption of the nerve fibre/ganglion cell layer (Figs 1, 2, 3; see text box). In addition, we detected marked retinal oedema especially in the nerve fibre/ganglion cell layer of the cone-rich zone near the optic nerve, the equivalent to the human macula (Figs 1, 2, 3; see text box).

Ocular lesions in INS^{C94Y} pigs

Site	Ocular findings in diabetic INS^{C94Y} transgenic pigs	Ocular correlates/diagnostic entities of diabetes mellitus in humans
Lens	Cataract	Cataract
Retina	Diabetic retinopathy with: • Vessel calibre irregularity • Tortuosity of vessels • Loop formation of capillaries • Extraretinal haemorrhage • Cotton-wool spots • Hard exudates in retina • Retinal oedema near optic nerve in cone-rich zone	Diabetic retinopathy with: • Intraretinal microvascular abnormalities • Proliferative diabetic retinopathy • Diabetic maculopathy • Diabetic macular oedema
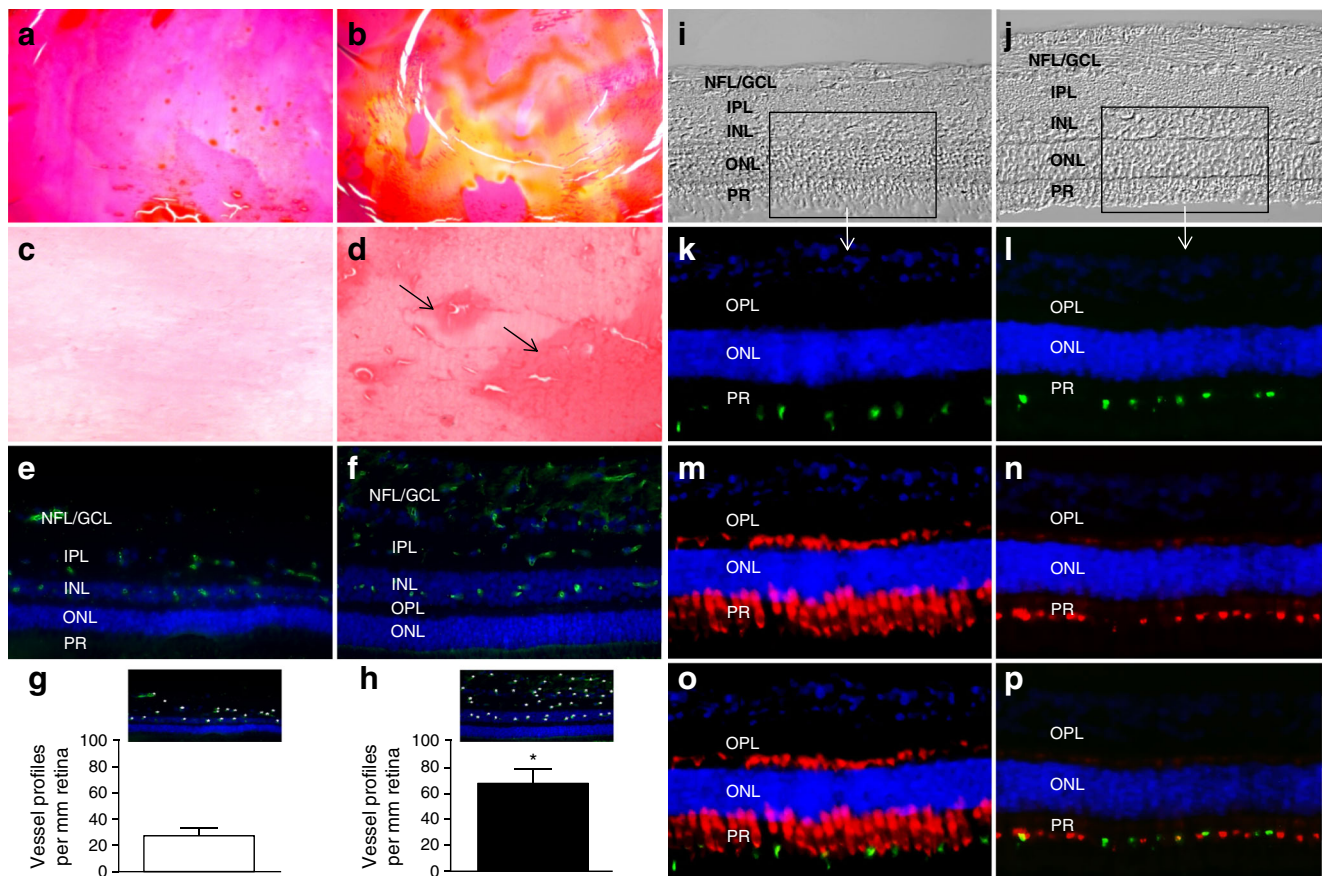
Fig. 2 INS^{C94Y} pigs have mature cataracts, tortuous vessels and altered protein expression patterns in morphologically intact cones. (**a**) The normal lens of a control pig; and (**b**) the lens of an INS^{C94Y} pig with a central cataract (×5, Mallory's stain). (**c**) The normal lens of a control pig; and (**d**) accumulation of eosinophilic material (arrows) in an INS^{C94Y} pig with a cataract (×10, H&E staining). The vessel endothelial marker LEL (green) in (**e**) a control and (**f**) an INS^{C94Y} pig identified a greater number of blood vessel section profiles and tortuous blood vessels in the retina of the INS^{C94Y} pig (×20 magnification). The number of blood vessel section profiles counted in 1 mm retina of (**g**) control and (**h**) INS^{C94Y} pigs ($n = 3$ per group, vessels stained with LEL) was significantly higher in diabetic pigs. Insets show representative counts. *$p < 0.05$. Stars indicate counted vessel profiles. Differential interference contrast image of (**i**) a healthy pig retina and (**j**) the retina of an INS^{C94Y} pig (×20 magnification). The box indicates the area that is shown with higher magnification in images (**k**–**p**). S-opsin (green) staining indicated no difference in the number of blue cones in (**k**) healthy control and (**l**) INS^{C94Y} pigs. Concurrent staining of cone arrestin revealed marked differences in the levels of cone arrestin expression (red) in the retinas of (**m**) control and (**n**) INS^{C94Y} pigs. (**o**) Healthy control and (**p**) INS^{C94Y} pigs: overlay (yellow) images of S-opsin and cone arrestin (×63 magnification). Cell nuclei: blue (DAPI). INL, inner nuclear layer; IPL, inner plexiform layer; NFL/GCL, nerve fibre/ganglion cell layer; ONL, outer nuclear layer; OPL, outer plexiform layer; PR, photoreceptors

Discussion

There is an urgent need for adequate animal models that mimic the important features of diabetic retinopathy. The importance of large-animal models is evolving, given their remarkable resemblance to the anatomical, physiological and pathological characteristics of many diseases in humans, such as diabetic retinopathy. The major sight-threatening complication of this disease is macular oedema [1]. Animal models for investigating certain features of this condition exist [5–7, 22] but, for greater translational value to humans, more suitable animal models, featuring as many hallmark pathologies observed in the human disease condition as possible, are urgently needed. In this study, we characterised the ocular phenotype of an INS^{C94Y} pig model of long-term diabetes mellitus (≥24 months). All INS^{C94Y} pigs showed several typical ocular lesions of diabetes mellitus (see text box), such as cataracts and severe retinopathy. Cataracts developed in the very early stages of diabetes mellitus in these pigs [11] and progressed to mature cataracts in all cases analysed.

Interestingly, the retinas of INS^{C94Y} pigs revealed significant changes in retinal architecture and the levels of functionally relevant proteins. There was a very prominent increase in retinal thickness in diabetic INS^{C94Y} pigs (Fig. 1), which was particularly confined to the regions 2 and 3 mm from the optic nerve, where pigs have a region of similar cellular composition to the macula in humans [5]. Closer examination of the affected retinal layers revealed that INS^{C94Y} pigs developed retinal oedema with a spatial distribution similar to that seen in humans with macular oedema [23]. An increase in the mean
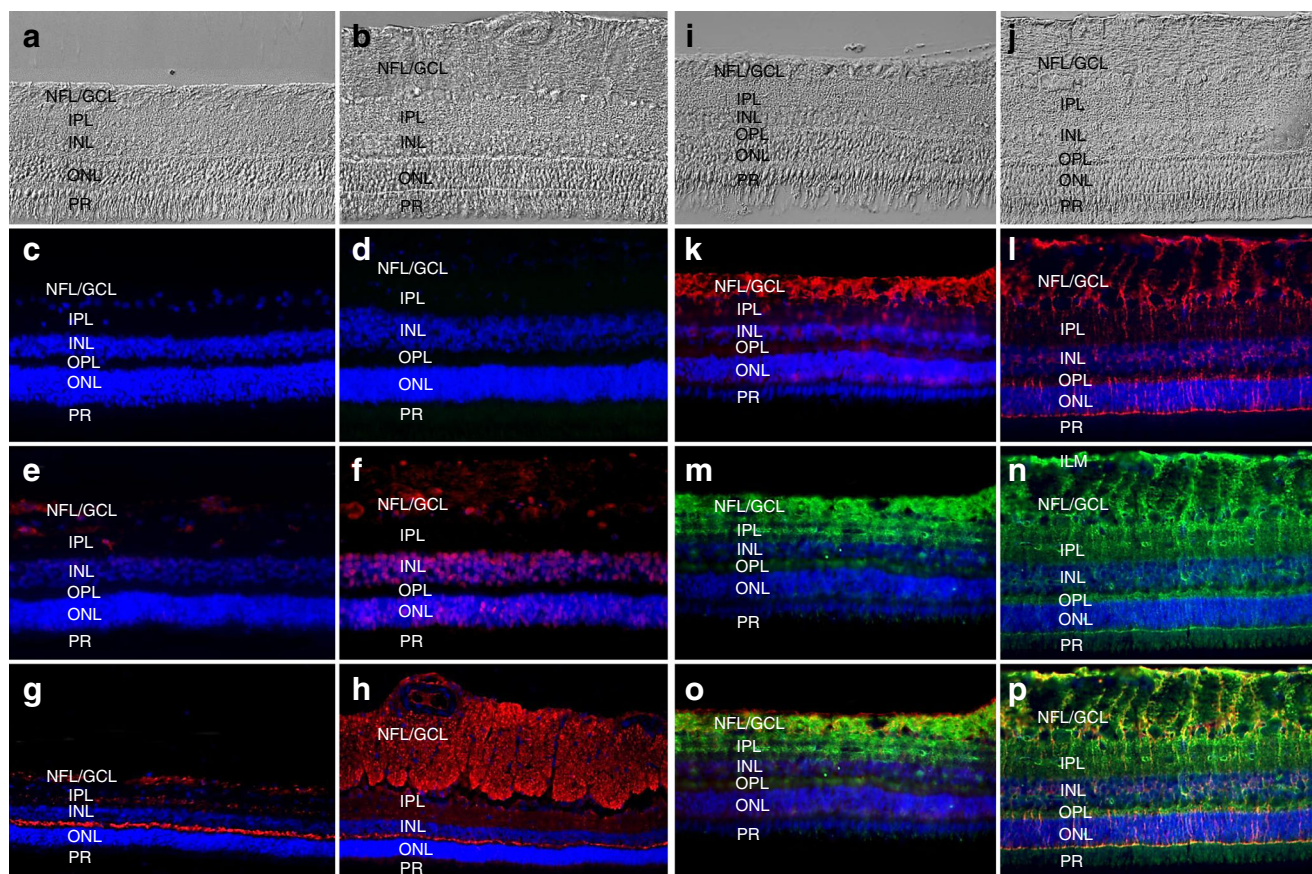
Fig. 3 In the retinas of diabetic *INS*[C94Y]pigs, IRS1 is highly phosphorylated at tyrosine residue 895, but not at serine 302_307. The increase in retinal thickness can be attributed to swelling of the nerve fibre/ganglion cell layer, and the major water channel of the retina, AQP4, has an altered structure in diabetes. Differential interference contrast images of retinas from (**a**) healthy and (**b**) *INS*[C94Y]pigs. No phosphorylation of IRS1 was detectable at serine residues 302 or 307 in (**c**) healthy control or (**d**) *INS*[C94Y]pigs (pIRS1 Ser302_307, red), whereas there was a marked difference in the abundance of pIRS1 at tyrosine residue 895 between (**e**) control and (**f**) *INS*[C94Y]pigs (pIRS1 Tyr 895, red). NEFH levels (red) in (**g**) healthy pig retina and (**h**) markedly increased levels in *INS*[C94Y]pig retina indicates an enlargement of neurons/axons in the nerve fibre/ganglion cell layer. Differential interference contrast image of the retinas of (**i**) healthy and (**j**) *INS*[C94Y]pigs. Specific labelling (GS; red) of (**k**) Müller glial cell endfeet in control pigs and (**l**) entire Müller glial cells in *INS*[C94Y]pigs. The main water channel of the retina, AQP4 (green), was less abundant in the retinas of (**m**) control vs (**n**) *INS*[C94Y]pigs, and shows a similar Müller glial cell specific pattern as GS. In addition, changes in AQP4 in *INS*[C94Y]pigs were especially prominent at the inner limiting membrane. Overlay images of GS and AQP4 in (**o**) control and (**p**) *INS*[C94Y]pigs confirmed Müller glial cell specific levels of AQP4 and additional levels in the inner and outer plexiform layers of control and *INS*[C94Y]retinas, (a–p: ×20 magnification). Cell nuclei: blue (DAPI). INL, inner nuclear layer; IPL, inner plexiform layer; NFL/GCL, nerve fibre/ganglion cell layer; ONL, outer nuclear layer; OPL, outer plexiform layer; PR, photoreceptors

central thickness of 1 mm in individuals with diabetic retinopathy defines a centre involving diabetic macular oedema, and this central thickness is correlated with the decrease in visual acuity [24].

In addition, typical vascular abnormalities (i.e. intraretinal microvascular abnormalities) of human diabetic retinopathy [20] were seen in the retinas of diabetic *INS*[C94Y]pigs. Retinal vessel calibre changes are associated with complications in humans with diabetes [25], and there is a consistent relationship between wider retinal venular calibres, lower fractal dimensions and the progression to proliferative retinopathy [26].

Furthermore, *INS*[C94Y]pigs developed typical irregularities at the inner limiting membrane, resulting in disruption of this barrier with the accumulation of hard exudates and cotton-wool spots, which are characteristic features of proliferative diabetic retinopathy. This is the most common microvascular end-stage complication, with a 16-year incidence of 31% in type 1 diabetes [26] and 15% in type 2 diabetes (over 20 years) [27]. The duration of diabetes is the strongest predictor for the development and progression of retinopathy, and models with longevity are therefore favourable [28]. A further advantage of the *INS*[C94Y]pig model is that all major complications were detectable after 2 years, which is very rapid compared with other large-animal models such as large primates, where the development of these signs has required more than 15 years [21].

Interestingly, *INS*[C94Y]pigs revealed an altered abundance of proteins important for colour vision. Impaired colour vision is a common observation in individuals with diabetic

retinopathy, starting in early, uncomplicated stages and increasing with macular oedema, in which two-thirds of individuals have colour discrimination abnormalities [29]. Some unique features of the INS^{C94Y}pig model, such as alterations in cones (Fig. 2k–p; text box), are replicated in other existing animal models, such as marmosets [22] and rats [6, 7].

Disruption of the inner limiting membrane in INS^{C94Y}pigs points to changes in Müller glial cell function. This was further substantiated by changes in proteins with important functions for Müller glial cell metabolism (e.g. GS) and the major retinal water channel protein AQP4 [30]. The development of retinal oedema is associated with Müller glial cell dysfunction in osmotic glial swelling [31], and the finding of similar alterations in diabetic INS^{C94Y}pigs therefore points to a similar pathophysiology. Müller cells are particularly important for retinal protective responses under stressful conditions [32]. AQP4 has been described in Müller cell (endfoot) membranes of pigs [33] and is involved in retinal volume regulation [28]. The observed alterations in GS and AQP4 levels (Fig. 3) in diabetic INS^{C94Y}pigs merit future investigation to clarify the potential role of Müller glial cells in oedema formation. Because of the similar function of pig and human Müller cells (e.g. both possess Ca^{2+}-activated K^+ channels), which are not ubiquitously present in all species [28], the pig is a good model in which to study these alterations.

This study represents a unique possibility to analyse the ocular consequences of long-term exposure (>2 years) to hyperglycaemia. The pig model replicates several hallmarks of diabetic retinopathy observed in humans (text box) that, to our knowledge, have not previously been found combined in one animal model. Marmosets (*Callithrix jacchus*) maintained on a 30% galactose-rich diet for 2 years have been reported to develop characteristic retinal vascular lesions with macular oedema and morphological characteristics, including acellular capillaries and pericyte loss, vessel tortuosity and capillary basement membrane thickness [22]. The findings from that study indicated that hyperhexosaemia triggered retinal vascular changes similar to those in human diabetic retinopathy; however, changes in cones or Müller glial cells were not described [22]. In the INS^{C94Y}pig model, longevity and physiological (e.g. Müller glial cell function) and anatomical similarities (a central, cone-rich area) with the human retina enabled specialised studies of these aspects.

Clearly, one limitation of this study was the monitoring of only one time point, presumably representing late-stage retinopathy, because we sampled at the endpoint of a long-term study designed to generate the first INS^{C94Y}pig biobank [34]. Therefore, we have no information on how rapidly pathophysiological features develop in the pig, and comparison with the disease dynamics of other models is limited. In future studies, investigation of the dynamics of diabetic retinopathy features should include an in vivo imaging technique such as optical coherence tomography, which is already standard when monitoring rodent models for diabetic retinopathy [6, 7]. However, this has yet to be established in the pig and the very early, severe cataract formation involving the entire lens with opacity at 4.5 months requires surgical removal of the lens prior to in vivo imaging [11]. If the changes develop after only months then this would be a drawback for the model, because it would make it impractical for several applications. The next step is to analyse earlier time points and, as cataract development starts as early as day 8 after birth [11], we hypothesise that other pathologies will also appear at an early point.

In summary, we confirmed our hypothesis by showing that the retinal changes occurring in the INS^{C94Y}pig make it an interesting and valuable model for further studies of diabetic retinopathy and its pathophysiology, and of proliferative diabetic retinopathy, intraretinal microvascular abnormalities or macular oedema risk stratification, and novel treatment strategies.

References

1. Kharroubi AT, Darwish HM (2015) Diabetes mellitus: the epidemic of the century. World J Diab 6:850–867
2. Ponto KA, Koenig J, Peto T et al (2016) Prevalence of diabetic retinopathy in screening-detected diabetes mellitus: results from the Gutenberg Health Study (GHS). Diabetologia 59:1913–1919
3. Tan GS, Cheung N, Simo R, Cheung GC, Wong TY (2017) Diabetic macular oedema. Lancet Diabetes Endocrinol 5:143–155

4. Antonetti DA, Barber AJ, Bronson SK et al (2006) Diabetic reti-
   nopathy: seeing beyond glucose-induced microvascular disease.
   Diabetes 55:2401–2411

5. Jiang X, Yang L, Luo Y (2015) Animal models of diabetic retinop-
   athy. Curr Eye Res 40:761–771

6. Berkowitz BA, Bissig D, Ye Y, Valsadia P, Kern TS, Roberts R
   (2012) Evidence for diffuse central retinal edema in vivo in diabetic
   male Sprague Dawley rats. PLoS One 7:e29619

7. Clermont A, Chilcote TJ, Kita T et al (2011) Plasma kallikrein
   mediates retinal vascular dysfunction and induces retinal thickening
   in diabetic rats. Diabetes 60:1590–1598

8. Huber G, Heynen S, Imsand C et al (2010) Novel rodent models for
   macular research. PLoS One 5:e13403

9. Hendrickson A, Hicks D (2002) Distribution and density of
   medium- and short-wavelength selective cones in the domestic
   pig retina. Exp Eye Res 74:435–444

10. Chandler MJ, Smith PJ, Samuelson DA, MacKay EO (1999)
    Photoreceptor density of the domestic pig retina. Vet Ophthalmol
    2:179–184

11. Renner S, Braun-Reichhart C, Blutke A et al (2013) Permanent
    neonatal diabetes in INS(C94Y) transgenic pigs. Diabetes 62:
    1505–1511

12. Albl B, Haesner S, Braun-Reichhart C et al (2016) Tissue sampling
    guides for porcine biomedical models. Toxicol Pathol 44:414–420

13. Wolf E, Braun-Reichhart C, Streckel E, Renner S (2014)
    Genetically engineered pig models for diabetes research.
    Transgenic Res 23:27–38

14. Chou J, Rollins S, Fawzi AA (2014) Role of endothelial cell and
    pericyte dysfunction in diabetic retinopathy: review of techniques
    in rodent models. Adv Exp Med Biol 801:669–675

15. Higgins PJ, Garlick RL, Bunn HF (1982) Glycosylated hemoglobin
    in human and animal red cells. Role of glucose permeability.
    Diabetes 31:743–748

16. Garca M, Ruiz-Ederra J, Hernandez-Barbachano H, Vecino E
    (2005) Topography of pig retinal ganglion cells. J Comp Neurol
    486:361–372

17. Amann B, Kleinwort KJ, Hirmer S et al (2016) Expression and
    distribution pattern of aquaporin 4, 5 and 11 in retinas of 15 differ-
    ent species. Int J Mol Sci 17:E1145

18. Amann B, Hirmer S, Hauck SM, Kremmer E, Ueffing M, Deeg CA
    (2014) True blue: S-opsin is widely expressed in different animal
    species. J Anim Physiol Anim Nutr (Berl) 98:32–42

19. Lavin DP, White MF, Brazil DP (2016) IRS proteins and diabetic
    complications. Diabetologia 59:2280–2291

20. Stitt AW, Curtis TM, Chen M et al (2016) The progress in under-
    standing and treatment of diabetic retinopathy. Prog Retin Eye Res
    51:156–186

21. Robinson R, Barathi VA, Chaurasia SS, Wong TY, Kern TS (2012)
    Update on animal models of diabetic retinopathy: from molecular ap-
    proaches to mice and higher mammals. Dis Model Mech 5:444–456

22. Chronopoulos A, Roy S, Beglova E, Mansfield K, Wachtman L,
    Roy S (2015) Hyperhexosemia-induced retinal vascular pathology
    in a novel primate model of diabetic retinopathy. Diabetes 64:2603–
    2608

23. Vujosevic S, Midena E (2013) Retinal layers changes in human
    preclinical and early clinical diabetic retinopathy support early ret-
    inal neuronal and Muller cells alterations. J Diabetes Res 2013:
    905058

24. Diabetic Retinopathy Clinical Research Network (2011) Rationale
    for the diabetic retinopathy clinical research network treatment pro-
    tocol for center-involved diabetic macular edema. Ophthalmology
    118:e5–e14

25. Broe R, Rasmussen ML, Frydkjaer-Olsen U et al (2014) Retinal
    vessel calibers predict long-term microvascular complications in
    type 1 diabetes: the Danish Cohort of Pediatric Diabetes 1987
    (DCPD1987). Diabetes 63:3906–3914

26. Broe R (2015) Early risk stratification in pediatric type 1 diabetes.
    Acta Ophthalmol 93(Thesis 1):1–19

27. Yau JW, Rogers SL, Kawasaki R et al (2012) Global prevalence and
    major risk factors of diabetic retinopathy. Diabetes Care 35:556–564

28. Fong DS, Aiello L, Gardner TW et al (2004) Retinopathy in diabe-
    tes. Diabetes Care 27(Suppl 1):S84–S87

29. Chous AP, Richer SP, Gerson JD, Kowluru RA (2016) The diabetes
    visual function supplement study (DiVFuSS). Br J Ophthalmol
    100:227–234

30. Pannicke T, Ivo Chao T, Reisenhofer M, Francke M, Reichenbach
    A (2017) Comparative electrophysiology of retinal Müller glial
    cells—a survey on vertebrate species. Glia 65:533–568

31. Pannicke T, Iandiev I, Wurm A et al (2006) Diabetes alters osmotic
    swelling characteristics and membrane conductance of glial cells in
    rat retina. Diabetes 55:633–639

32. Sorrentino FS, Allkabes M, Salsini G, Bonifazzi C, Perri P (2016)
    The importance of glial cells in the homeostasis of the retinal mi-
    croenvironment and their pivotal role in the course of diabetic ret-
    inopathy. Life Sci 162:54–59

33. Iandiev I, Uckermann O, Pannicke T et al (2006) Glial cell reactiv-
    ity in a porcine model of retinal detachment. Investig Ophthalmol
    Vis Sci 47:2161–2171

34. Abbott A (2015) Inside the first pig biobank. Nature 519:397–398